Induced superconductivity in noncuprate layers of the $Bi_2Sr_2CaCu_2O_{8+\delta}$ high-temperature superconductor: Modeling of scanning tunneling spectra

Ilpo Suominen
Department of Physics, Tampere University of Technology, P.O. Box 692, FIN-33101 Tampere, Finland

Jouko Nieminen*
Department of Physics, Tampere University of Technology, P.O. Box 692, FIN-33101 Tampere, Finland and
Department of Physics, Northeastern University, Boston, Massachusetts 02115, USA

R. S. Markiewicz and A. Bansil
Department of Physics, Northeastern University, Boston, Massachusetts 02115, USA
(Received 15 September 2010; published 4 January 2011)

We analyze how the coherence peaks observed in scanning tunneling spectroscopy (STS) of cuprate high-temperature superconductors are transferred from the cuprate layer to the oxide layers adjacent to the STS microscope tip. For this purpose, we have carried out a realistic multiband calculation for the superconducting state of $Bi_2Sr_2CaCu_2O_{8+\delta}$ (Bi2212) assuming a short-range d-wave pairing interaction confined to the nearest-neighbor Cu $d_{x^2-y^2}$ orbitals. The resulting anomalous matrix elements of the Green's function allow us to monitor how pairing is then induced not only within the cuprate bilayer but also within and across other layers and sites. The symmetry properties of the various anomalous matrix elements and the related selection rules are delineated.

DOI: 10.1103/PhysRevB.83.024501 PACS number(s): 68.37.Ef, 71.20.−b, 74.50.+r, 74.72.−h

I. INTRODUCTION

Scanning tunneling spectra (STS) of the cuprates[1–5] clearly show the presence of superconducting gaps and the associated coherence peaks. The "leaking" of superconductivity from the cuprate layers into the oxide layers is a form of proximity effect.[6–8] A recent STS study[9] finds that the magnitude of the superconducting gap or the pseudogap is not solely determined by the local doping, but is also sensitive to the nearby nanoscale surroundings, raising the broader question as to how superconductivity is transferred across various orbitals and/or sites in the cuprates.[10] In this connection, we have recently developed a Green's-function-based methodology for carrying out realistic computation of scanning tunneling microscopy–scanning tunneling spectroscopy (STM-STS) spectra in the normal state as well as the superconducting state of complex materials, where the nature of the tunneling process, i.e., the effect of the tunneling matrix element is properly taken into account. In our approach, all relevant orbitals in the material are included in a multiband framework, and the tunneling current is computed directly for a specific tip position on the semi-infinite surface of the solid. An application to the case of overdoped Bi2212 was reported in Refs. 11 and 12, where it was shown, for example, that the striking asymmetry of the STS spectrum between high positive- and negative-bias voltages arises from the way electronic states in the cuprate layer couple to the tip: With increasing negative-bias voltage, new tunneling channels associated with d_{z^2} and other orbitals begin to open up to yield the large tunneling current. The asymmetry of the tunneling current at high energies could thus be understood naturally within the conventional picture, without the need to invoke exotic mechanisms. Results of Refs. 11 and 12 show clearly that the STS spectrum is modified strongly by matrix-element effects, as has been shown previously for angle-resolved photoemission,[13] resonant inelastic x-ray scattering,[14] and other highly resolved spectroscopies.[15–17]

The STM-STS modeling in Refs. 11 and 12 is based on invoking the common assumption that the pairing interaction in cuprates is d wave, involving nearest-neighbor $d_{x^2-y^2}$ orbitals of Cu atoms. Nevertheless, our computed STS spectrum reproduces, in accord with experimental observations, the superconducting gap and coherence peaks at the position of the tip, even though the tip is not in direct contact with the cuprate layer. Our STS modeling scheme thus provides a natural basis for examining how the pairing interaction, which is limited to nearest-neighbor Cu $d_{x^2-y^2}$ orbitals in our underlying Hamiltonian, gets transferred to other layers and sites.

This article attempts to address these and related issues with the example of overdoped Bi2212. Central to our analysis is the concept of tunneling channels, which allows us to identify the contribution to the total tunneling current from individual sites and/or orbitals in the semi-infinite solid. Moreover, we can distinguish between regular and anomalous contributions to the tunneling signal, which arise from the corresponding matrix elements of the Nambu-Gorkov Green's-function tensor. The anomalous channels are physically related to the formation and breaking up of Cooper pairs. In particular, matrix elements of the anomalous Green's function can be used to monitor the contribution to the coherence peaks in the STS spectrum resulting from specific orbitals and/or sites in the material. In this way, we delineate how the pairing amplitude travels from the nearest-neighbor Cu sites to other sites and orbitals within the cuprate plane as well as outside to the second cuprate plane and to the BiO/SrO layers. The symmetry properties of various matrix elements are analyzed and related selection rules are worked out.

An outline of this article is as follows. The introductory remarks are followed in Sec. II with an overview of the relevant

methodological details of the underlying Hamiltonian and of our STS formalism. Section III discusses proximity effects and is divided into several subsections, which address pairing amplitudes in various layers. Section IV discusses selection rules and issues related to the symmetry of the gap through an analysis of the anomalous matrix elements. It is divided into consideration of on-site cases where the pairing orbitals lie at the same horizontal position, and to cases where these orbitals lie at other sites in the lattice. Finally, Sec. V presents a concluding discussion and a summary of our results. The Appendix clarifies the symmetry properties of the regular matrix elements, which play an important role in the analysis of the symmetry of the anomalous matrix elements of the Green's function.

II. DESCRIPTION OF THE MODEL

The model underlying our analysis is the same as in Ref. 12, to which we refer for details. An overview is nevertheless presented for completeness, and to introduce the various quantities needed for the present study. The Bi2212 sample is modeled as a slab of seven layers terminated by the BiO layer, which is followed by layers of SrO, CuO_2, Ca, CuO_2, SrO, and BiO.[18–20] The tunneling current is computed by using a $2\sqrt{2} \times 2\sqrt{2}$ real-space supercell consisting of eight primitive surface cells with a total of 120 atoms. The crystal structure is taken from Ref. 21. The STM tip is modeled as an s orbital lying at the apex of the tip. The electron and hole orbitals included in the computations are as follows: (s, p_x, p_y, p_z) for Bi, Ca, and O; s for Sr; and $(4s, d_{3z^2-r^2}, d_{xy}, d_{xz}, d_{yz}, d_{x^2-y^2})$ for Cu atoms. This yields 2×58 electron (spin-up) and hole (spin-down) orbitals in the primitive unit cell, or a total of 2×464 orbitals in the simulation supercell. The Green's function is computed by using 256 equally distributed $\mathbf{k}$ points in the supercell, which corresponds to $8 \times 256 = 2048$ $\mathbf{k}$ points in a primitive cell.

The multiband Hamiltonian in which superconductivity is included by adding a pairing interaction term Δ is[22–24]

$$\hat{H} = \sum_{\alpha\beta\sigma} (\varepsilon_\alpha c^\dagger_{\alpha\sigma} c_{\alpha\sigma} + V_{\alpha\beta} c^\dagger_{\alpha\sigma} c_{\beta\sigma}) + \sum_{\alpha\beta\sigma} (\Delta_{\alpha\beta} c^\dagger_{\alpha\sigma} c^\dagger_{\beta-\sigma} + \Delta^\dagger_{\beta\alpha} c_{\beta-\sigma} c_{\alpha\sigma}), \quad (1)$$

with real-space creation (annihilation) operators $c^\dagger_{\alpha\sigma}$ (or $c_{\alpha\sigma}$). Here α is a composite index identifying both the type of orbital and its site, and σ is the spin index. ε_α denotes the on-site energy of the αth orbital, and $V_{\alpha\beta}$ is the hopping integral between the α and β orbitals. The hopping parameters are chosen to reproduce the local-density approximation (LDA) bands.[25–29]

In the mean-field approximation, the coupling between electrons and holes is of the form

$$\Delta_{\alpha\beta} = \sum_{ab} U_{\alpha\beta ab} \langle c_{a\downarrow} c_{b\uparrow} \rangle. \quad (2)$$

Because the interaction U is not known, the standard practice is to introduce a gap parameter, which gives the correct gap width and symmetry.[30] Specifically, we take Δ to be nonzero only between the $d_{x^2-y^2}$ orbitals of the nearest-neighbor Cu atoms, and to possess a d-wave form, i.e., $\Delta_{d(d\pm x)} = +|\Delta|$ and $\Delta_{d(d\pm y)} = -|\Delta|$, where d denotes the $d_{x^2-y^2}$ orbital at a chosen site, and $d \pm x\,(y)$ is the $d_{x^2-y^2}$ orbital of the neighboring Cu atom in the x-y direction.[31] This form allows electrons of opposite spins to combine to produce superconducting pairs such that the resulting superconducting gap is zero along the nodal directions $k_x = \pm k_y$, and is maximum along the antinodal directions. The gap parameter value of $|\Delta| = 45$ meV is chosen to model a typical experimental spectrum[2] for our illustrative purposes.[32,33]

We discuss pairing between different orbitals in terms of the tensor (Nambu-Gorkov) Green's function $\mathcal{G}$ (see, e.g., Ref. 34),

$$\mathcal{G} = \begin{pmatrix} G_e & F \\ F^\dagger & G_h \end{pmatrix},$$

where G_e and G_h denote the electron and hole Green's function, respectively.

The following expressions for the pairing amplitudes in a tight-binding basis, which are derived in Ref. 12, are especially relevant for our analysis:

$$\langle c_{\alpha\downarrow} c_{\beta\uparrow} \rangle = \int d\varepsilon [1 - 2f(\varepsilon)] \rho^{eh}_{\alpha\beta}(\varepsilon), \quad (3)$$

where the density matrix is

$$\rho^{eh}_{\alpha\beta}(\varepsilon) = -\frac{1}{\pi} \mathrm{Im}[F^+_{\alpha\beta}(\varepsilon)].$$

Here, $F^+_{\alpha\beta}(\varepsilon)$ can be solved by using the tensor form of Dyson's equation for the retarded Green's function. Similarly,

$$\langle c^\dagger_{\alpha\uparrow} c^\dagger_{\beta\downarrow} \rangle = \int d\varepsilon [1 - 2f(\varepsilon)] \rho^{eh\dagger}_{\beta\alpha}(\varepsilon). \quad (4)$$

Equations (3) and (4) reveal the relationship between the anomalous part of the Green's-function tensor and the pairing amplitudes between various sites. In particular, symmetry properties of $F_{\alpha\beta}$ are seen to be related directly to those of $\langle c_{\alpha\downarrow} c_{\beta\uparrow} \rangle$.

The tunneling spectrum is computed by using the Todorov-Pendry expression[35,36] for the differential conductance σ between orbitals of the tip (t,t') and the sample (s,s'), which in our case can be written as

$$\sigma = \frac{dI}{dV} = \frac{2\pi e^2}{\hbar} \sum_{tt'ss'} \rho_{tt'}(E_F) V_{t's} \rho_{ss'}(E_F + eV) V^\dagger_{s't}. \quad (5)$$

Because electrons are not eigenparticles in the presence of the pairing term, the density matrix can be rewritten by applying the tensor form of the Dyson equation:[12]

$$\rho_{ss'} = -\frac{1}{\pi} \sum_\alpha (G^+_{s\alpha} \Sigma''_\alpha G^-_{\alpha s'} + F^+_{s\alpha} \Sigma''_\alpha F^-_{\alpha s'}), \quad (6)$$

where Σ''_α is the imaginary part of self-energy.[37,38] The left-hand side of Eq. (6) is the ordinary density matrix for electrons, which is equivalent to the traditional Tersoff-Hamann approach.[39] However, as discussed in Ref. 12, our decomposition of the spectrum into tunneling channels in Eq. (6) provides a powerful way to gain insight into the nature of the STS spectrum, especially in complex materials.[40,41] Note that the right-hand side of Eq. (6) contains terms originating

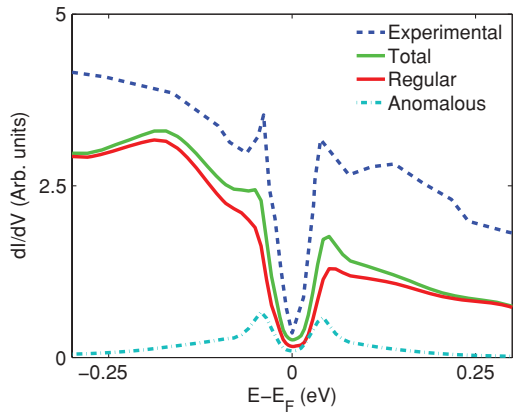

FIG. 1. (Color online) Theoretical (green) STS spectrum normalized as shown in the figure is compared with the experimental (dashed blue) spectrum (Ref. 2) in optimally doped Bi2212. Regular (red) and anomalous (turquoise) parts of the computed spectrum are shown separately. All computations are based on Eq. (6). Coherence peaks arise only from the anomalous component of the Green's function.

from the anomalous part of the Green's function. In Ref. 12 we showed that coherence peaks appear only through the matrix elements of the anomalous Green's function. This role of the anomalous terms is demonstrated in Fig. 1, where we see that the coherence peaks are absent in the partial spectrum resulting from the regular terms of the Green's function (red curve).

III. INTERLAYER AND INTRALAYER PROXIMITY EFFECTS

In this section, we analyze the induced pairing amplitude $\langle c_{\alpha\downarrow} c_{\beta\uparrow}\rangle$ for a representative set of orbitals. It will be seen that despite the short range of the pairing interaction $\Delta_{\alpha\beta}$, the anomalous Green's function, $F_{\alpha\beta}$, possesses a longer range.

TABLE I. Shorthand notation used for the indices α and β in Fig. 2 is defined. For each of the indices, varying from 0 to 9, the table gives the atomic site [central (c), nearest neighbor (nn), and bonding (b)], the orbital, and the layer involved. The order of the layers is as follows: BiO, SrO, CuO_2 (1st) and CuO_2 (2nd), where BiO is the termination layer that lies closest to the STM tip.

Label	Orbital	Atom	Layer
0	$d_{x^2-y^2}$	Cu (c)	CuO_2 (1st)
1	$d_{x^2-y^2}$	Cu (nn)	CuO_2 (2nd)
2	$d_{x^2-y^2}$	Cu (nn)	CuO_2 (2nd)
3	d_{z^2}	Cu (c)	CuO_2 (1st)
4	d_{z^2}	Cu (nn)	CuO_2 (1st)
5	p_z	O (c)	SrO
6	p_z	O (nn)	SrO
7	p_z	Bi (c)	BiO
8	p_z	Bi (nn)	BiO
9	p_x	O (b)	CuO_2 (1st)

More specifically, we delineate induced pairing effects as follows: (i) within a CuO_2 bilayer [Fig. 2(a)]; (ii) intralayer pairing in SrO and BiO layers [Fig. 2(b)]; and (iii) interlayer pairing between CuO_2 and SrO/BiO layers [Fig. 2(c)]. We discuss each of these cases in turn below with reference to Fig. 2 and Table I.

A. Pairing within the CuO_2 bilayer

The most important anomalous matrix elements within the CuO_2 bilayer are shown in Fig. 2(a). The red curve gives the contribution F_{01} from $d_{x^2-y^2}$ orbitals of two neighboring Cu atoms in the x direction, i.e., the matrix element between a spin-up electron orbital at a Cu site and a spin-down hole orbital at the neighboring Cu site. This is the principal pairing

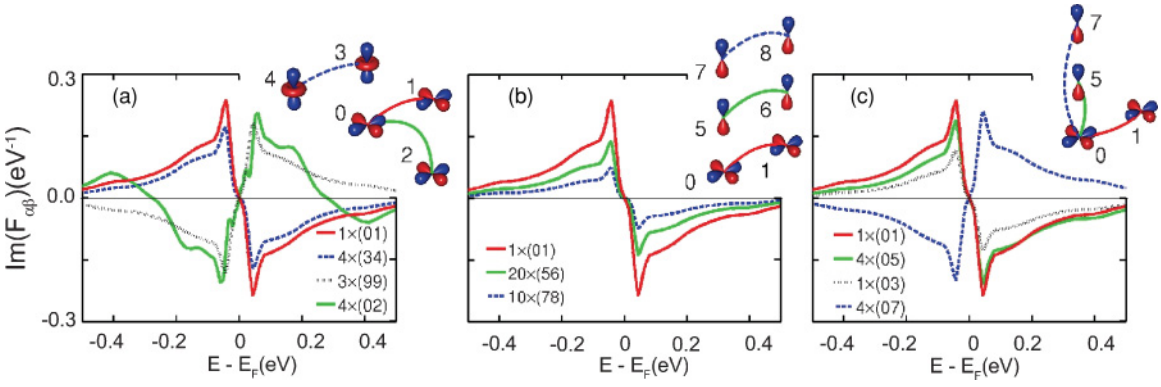

FIG. 2. (Color online) Imaginary part of the matrix elements of the anomalous Green's function $F_{\alpha\beta}$ for various $(\alpha\beta)$ pairs. (Recall that α and β are composite indices denoting both the site and the orbital.) The meaning of values of α and β, which range from 0 to 9, is explained in Table I. For example, index 0 refers to the $d_{x^2-y^2}$ orbital on the central Cu atom in the cuprate plane nearest to the STM tip, and index 1 refers to the $d_{x^2-y^2}$ orbital on the nearest-neighbor Cu atom in the same cuprate plane. The main matrix element between the two preceding orbitals, i.e., the (01) element, is shown by red lines for reference in all panels. Other matrix elements are shown scaled by factors ranging from 2 to 20, as indicated in the legends. Symmetries of the orbitals involved in various cases are shown schematically in the upper right-hand-side portions of the figures. Matrix elements compared with (01) (red curve) are as follows: (a) (02) (green curve), (34) (dashed blue curve), and (99) (dotted black curve) for pairing within a CuO_2 bilayer; (b) (56) (green curve) and (78) (dashed blue curve) for intralayer pairing in SrO and BiO layers; and (c) (03) (dotted black curve), (05) (green curve), and (07) (dashed blue curve) for pairing of CuO_2 along the line connecting the central Cu and the surface Bi.

matrix element because in our model $\Delta_{\alpha\beta}$ is nonzero only between two such orbitals.

The matrix element between the $d_{x^2-y^2}$ orbitals of two Cu atoms at the same horizontal position within the CuO_2 bilayer is zero by symmetry. However, the matrix element F_{02} between a Cu atom in the upper layer and each of the four neighboring Cu atoms of the lower layer (and vice versa) is seen from Fig. 2(a) to be substantial with an amplitude that is $\sim$0.25 of F_{01}. This result shows that pairing is not restricted to $d_{x^2-y^2}$ orbitals within a single CuO_2 layer, i.e., it is not two dimensional but extends vertically within the bilayer.

The d_{z^2} orbital of Cu also plays an important role. In fact, this orbital serves as a kind of gate for passing tunneling current from the cuprate layers to the SrO and BiO layers. Figure 2(a) shows that the amplitude F_{34} is $\sim$0.2 of F_{01} and comparable to F_{02}. There is also a smaller ($\sim$0.2 of F_{34}) rotationally invariant matrix element F_{04} (not shown in Fig. 2) between the d_{z^2} of a central Cu and the $d_{x^2-y^2}$ orbitals of the four neighboring Cu atoms. At first glance this seems to break the d-wave symmetry, but we will show below that the combined symmetry of the orbitals involved remains d wave.[42]

The role of O atoms in the cuprate layers can be delineated through the matrix elements F_{99} and F_{09}. In Fig. 2(a) we show the on-site matrix element F_{99}, which is $\sim$0.25 of the F_{01} term. We observe that in real-space rotations of $\pi/2$ around the central Cu, F_{99} changes its sign. A smaller contribution is found for F_{09} (not shown in Fig. 2). Its symmetry properties are consistent with the symmetry of the Zhang-Rice singlet, where a local orbital is constructed as a linear combination of the four oxygen atoms around the central Cu. The symmetry analysis of Sec. IV below shows that both F_{99} and F_{09} are also consistent with the d-wave symmetry.

Finally, we note that there is a substantial term, F_{03}, between the d_{z^2} and $d_{x^2-y^2}$ orbitals of *the same Cu atom*, which is perhaps surprising. Figure 2(c) shows that this pairing amplitude is about half of F_{01}. Because this is an on-site term, the d-wave symmetry again follows from the combined symmetry of the two orbitals, as discussed in Sec. IV below.

B. Intralayer pairing within SrO and BiO layers

In considering intralayer pairing in the SrO/BiO layers, we find that for Bi or apical O atoms, the most important nonzero anomalous matrix elements occur between p_z orbitals of the central atom and its four neighbours, i.e., F_{56} and F_{78}. These matrix elements possess the same d-wave symmetry as F_{01}. While all matrix elements have the same energy dependence in Fig. 2(b), F_{01} is $\sim$30$\times$ larger than F_{56} or F_{78}. The coherence peaks lie at exactly the same energy in each layer, i.e., the gap width is the same in all layers. The scaling factor for the amplitude seems to roughly follow the spectral weight of the orbitals. Hence, the pairing of electrons within the oxide layers seems to be a direct consequence of the tail of the CuO_2 electron-wave function within the various layers. This kind of pairing is in the spirit of the original idea of proximity effect,[6–8] where superconductivity is viewed as "leaking" from the superconducting part of the sample to the normal state material. Although the aformentioned orbitals are the most important ones, nonzero pairing is not restricted to just these orbitals. On the other hand, certain terms are strictly zero owing to symmetry. In particular, all the on-site F_{ss}, $F_{p_xp_x}$, $F_{p_yp_y}$, and $F_{p_zp_z}$ from Bi and O(Sr) are zero, as are many Bi-O(Bi) and O(Sr)-Sr terms. However, $F_{p_xp_y}$ of two neighboring Bi atoms is nonzero, as is $F_{p_xp_y}$ on the same Bi atom.

C. Interlayer pairing between CuO_2 and SrO/BiO layers

Pairing on BiO and SrO layers is not restricted to the intralayer terms discussed above. The interlayer terms F_{05} and F_{07} between the p_z orbitals of the central Bi [or O(Sr)] and $d_{x^2-y^2}$ of Cu *right below* these atoms is, in fact, significant, while the anomalous term to the neighboring Cu atoms is rather small. The existence of these matrix elements might be surprising, because the regular matrix elements are zero by symmetry between $d_{x^2-y^2}$ and the rotationally symmetric orbitals of the atoms above the central Cu (see the Appendix). But we will show in the following section that these matrix elements are not symmetry forbidden. From Fig. 2(c), the scaling factor between these elements and F_{01} is of the order of 4. Notably, this interlayer pairing would appear as k_z dependence in the gap function. If we make a reflection of the slab with respect to the Ca plane lying between the two CuO_2 layers, the corresponding anomalous matrix elements change their sign, indicating that this term has a node at $k_z = 0$, and thus deviations from d-wave symmetry should be found for nonzero k_z. The k_z dependence is also seen in the rather small terms between p_z orbitals of the Bi atoms of the surface layer, and the nearest-neighbor Bi atoms of the BiO layer with half the primitive cell below the surface.

IV. SYMMETRY AND SELECTION RULES FOR INDUCED PAIRING

We now discuss the symmetry properties and the related selection rules for the anomalous matrix elements of the Green's function in terms of the d-wave symmetry of the pairing matrix.

A. Symmetry properties of the anomalous matrix elements

Note first that the symmetry of the pair wave function depends on the relative motion of the pairing electrons, i.e., only on the relative coordinate $R_i - R_j$. The analysis of the symmetry properties, however, becomes more transparent in k space. Accordingly, we transform the real-space matrix elements $F_{i\alpha j\beta}(\varepsilon)$ into k space as

$$F_{\alpha\beta}(\mathbf{k},\varepsilon) = \sum_j \langle \mathbf{k}|0\,\alpha\rangle F_{0\alpha j\beta}(\varepsilon)\langle j\beta|\mathbf{k}\rangle$$
$$= \sum_j F_{0\alpha j\beta}(\varepsilon) e^{-i\mathbf{k}\cdot\mathbf{R_j}} \varphi^*_\alpha(\mathbf{k})\varphi_\beta(\mathbf{k}). \qquad (7)$$

Here, we have set $R_i = 0$ and $\varphi_\alpha(\mathbf{k})$ is the orbital wave function in k space. The site indices i and j and the orbital indices α and β are shown explicitly for all matrix elements. The summation is taken over the site index j. The orbital indices are obviously not involved in the transformation. For simplicity, we will restrict the analysis below such that j is either on site or one of the nearest neighbors of the central site. The generalization to further out neighbors is straightforward.

We need to take into account not only the phase difference between the sites, but also the form of the tight-binding orbitals $\varphi_\alpha(\mathbf{k})$. These orbitals have the same symmetry in real space and k space. In particular,

$$\begin{aligned}\varphi_x^*(\mathbf{k}) &= \langle \mathbf{k}|p_x\rangle \propto \frac{k_x}{k},\\ \varphi_y^*(\mathbf{k}) &= \langle \mathbf{k}|p_y\rangle \propto \frac{k_y}{k},\\ \varphi_{x^2-y^2}^*(\mathbf{k}) &= \langle \mathbf{k}|d_{x^2-y^2}\rangle \propto \frac{k_x^2-k_y^2}{k^2},\\ \varphi_{3z^2-r^2}^*(\mathbf{k}) &= \langle \mathbf{k}|d_{3z^2-r^2}\rangle \propto \frac{3k_z^2-k^2}{k^2}.\end{aligned} \tag{8}$$

The symmetry of the matrix elements is now readily analyzed. We give two examples to illustrate the procedure: (i) F_{01} between the $d_{x^2-y^2}$ orbitals of the central Cu and its neighbors, and (ii) F_{03} between d_{z^2} and $d_{x^2-y^2}$ at the central site. In the case of F_{01} the product of the orbital functions is even under rotations by $\pi/2$:

$$\varphi_\alpha^*(\mathbf{k})\varphi_\alpha(\mathbf{k}) = |\varphi_\alpha(\mathbf{k})|^2.$$

In fact, this applies to all cases where $\alpha = \beta$. Summing over the four sites around the central Cu and applying the odd parity with respect to $\pi/2$ rotation of the real-space matrix elements $F_{0\alpha j\alpha} \sim \Delta_{0j}$, we obtain

$$F_{\alpha\alpha}(\mathbf{k},\varepsilon) = 2|F_{0\alpha j\alpha}(\varepsilon)|[\cos(k_x a) - \cos(k_y a)]|\varphi_\alpha(\mathbf{k})|^2, \tag{9}$$

which is obviously d wave. This is easy to see for the $d_{x^2-y^2}$ orbitals, but Eq. (9) leads to the same conclusion for any set of four neighboring orbitals similar to the central one, as long as the real-space element is odd under rotations by $\pi/2$.

Turning to the case of F_{03}, here the sum in Eq. (7) consists of a single term (central site), so that there is no site-related phase factor. We only need to consider the product of orbitals:

$$\varphi_{3z^2-r^2}^*(\mathbf{k})\varphi_{x^2-y^2}(\mathbf{k}) \propto \frac{3k_z^2-k^2}{k^4}\left(k_x^2-k_y^2\right). \tag{10}$$

This is the only term through which angular dependence enters in Eq. (7). This again is d wave, keeping in mind that only the in-plane symmetry is relevant. These considerations apply more generally to any case where the two orbitals involved lie at the same horizontal position, with one of the orbitals being rotationally invariant and the other is d wave.

B. Selection rules for anomalous matrix elements

Selection rules for the matrix elements $F_{i\alpha j\beta}$ of the anomalous Green's function do not follow directly from those for the corresponding regular matrix elements discussed in the Appendix. For this purpose, we write $F_{i\alpha j\beta}$ as[12]

$$F_{i\alpha j\beta}(\varepsilon) = -G^+_{i\alpha k\gamma}(\varepsilon)\Delta_{k\gamma l\delta}G^{0-}_{l\delta j\beta}(-\varepsilon), \tag{11}$$

where the Einstein summation convention is implicit, and both the Green's functions on the right-hand side of the equation are regular. The first term is the renormalized Green's function for the superconducting state, while the second term with a superscript zero is the bare Green's function for the normal state. However, as shown in the Appendix, the symmetry properties of these two Green's functions are the same because both are regular.

Equation (11) highlights the central role of the pairing matrix $\Delta_{k\gamma l\delta}$ in determining the symmetry properties of $F_{i\alpha j\beta}$. However, summation over the intermediate states is cumbersome. Therefore, we convert Eq. (11) to k space first:

$$F(\mathbf{k},\varepsilon) = -G(\mathbf{k},\varepsilon)\Delta_{\mathbf{k}}G^{0*}(\mathbf{k},-\varepsilon), \tag{12}$$

where orbital indices are suppressed. Equation (12) makes it clear that $F(\mathbf{k},\varepsilon)$ possesses the d-wave symmetry of $\Delta_{\mathbf{k}}$ because the regular Green's functions are rotationally invariant, as shown in the Appendix.

Converting $F(\mathbf{k},\varepsilon)$ to the real space yields

$$F_{i\alpha j\beta}(\varepsilon) = \sum_{\mathbf{k}}\langle i\alpha|\mathbf{k}\rangle F(\mathbf{k},\varepsilon)\langle \mathbf{k}|j\beta\rangle \tag{13}$$

or

$$F_{0\alpha j\beta}(\varepsilon) = \sum_{\mathbf{k}} e^{i(k_z z_j + k_\parallel\cdot R_{\parallel j})}\varphi_\alpha^*(\mathbf{k})\varphi_\beta(\mathbf{k})F(\mathbf{k},\varepsilon), \tag{14}$$

where we have fixed the first site index to $R_i = 0$, and made a separation into perpendicular ($k_z z_j$) and parallel directions ($k_x x_j + k_y y_j = k_\parallel\cdot R_{\parallel j}$).

We first consider the case where orbitals α and β are at the same horizontal site, i.e., $R_{\parallel j} = 0$. The necessary condition for the matrix element $F_{0\alpha j\beta}$ to be nonzero is that

$$\varphi_\alpha^*(\mathbf{k})\varphi_\beta(\mathbf{k})F(\mathbf{k},\varepsilon) \tag{15}$$

is rotationally invariant. Because $F(\mathbf{k},\varepsilon)$ is d wave, the product of wave functions on the right-hand side of Eq. (14) must have d-wave symmetry. For example, one of the orbitals could be d-wave symmetric and the other could be rotationally invariant. In particular, the anomalous matrix element between $d_{x^2-y^2}$ and one of the set $\{s, p_z, d_{z^2}\}$ satisfies this condition.

Furthermore, if $z_j = 0$, i.e., the orbitals are at the same site, the term in Eq. (15) must also have an even parity in the z direction for a nonzero matrix element, and hence p_z would not be a possible pair with $d_{x^2-y^2}$. However, in the case of $z_j \neq 0$, p_z is allowed, because the phase factor $e^{ik_z z_j}$ does not have a well-defined parity. Note also that the anomalous matrix element between $d_{x^2-y^2}$ orbitals at the same horizontal position ($R_{\parallel j} = 0$) is necessarily zero, because the term in Eq. (15) is odd under rotations of $\pi/2$.

We next consider matrix elements between orbitals at neighboring sites where $R_{\parallel j} = x_j = \pm a$ or $R_{\parallel j} = y_j = \pm a$. In this case, we will see that there will always be a nonzero matrix element with a properly symmetrized combination of neighboring wave functions, and the selection rules determine the correct choice of phase factors between sites. We discuss a particular case in detail as an example. Specifically, let us compare sites $R_j = (a,0,c)$ and $R_l = (0,a,c)$ and check whether or not the sign of the sum in Eq. (14) changes. For the first site we get

$$F_{0\alpha j\beta} = \sum_{\mathbf{k}} e^{i(k_x a + k_z c)}\varphi_\alpha^*(k_x,k_y)\varphi_\beta(k_x,k_y)F(\mathbf{k},\varepsilon) \tag{16}$$

and for the second site we get

$$F_{0\alpha l\beta} = \sum_{\mathbf{k}} e^{i(k_y a + k_z c)}\varphi_\alpha^*(k_x,k_y)\varphi_\beta(k_x,k_y)F(\mathbf{k},\varepsilon). \tag{17}$$

A rotation of $\pi/2$ is equivalent to the transformation $k_y \to k_x$ and $k_x \to -k_y$. Applying this to Eq. (17) yields

$$F_{0\alpha l\beta} = \sum_{\mathbf{k}} e^{i(k_x a + k_z c)} \varphi^*_\alpha(-k_y,k_x)\varphi_\beta(-k_y,k_x) F(\mathbf{k},\varepsilon). \quad (18)$$

Thus the product $\varphi^*_\alpha(-k_y,k_x)\varphi_\beta(-k_y,k_x)$ determines what happens under rotations of $\pi/2$ around the site $i = 0$. There are two cases: (1) This product is equal to $\varphi^*_\alpha(k_x,k_y)\varphi_\beta(k_x,k_y)$, so that these terms are invariant, and the total effect of rotation on $F_{0\alpha j\beta}$ in Eq. (14) follows the d-wave symmetry of $F(\mathbf{k},\varepsilon)$; and (2) the products of the orbitals in k space have the opposite sign, and the matrix element $F_{0\alpha j\beta}$ is invariant under in-plane rotation by $\pi/2$. In either case there will be pairing between the central orbital α and a properly symmetrized orbital ϕ, as defined in Eq. (A6) of the Appendix. For case (1), an invariant $\varphi^*_\alpha(k_x,k_y)\varphi_\beta(k_x,k_y)$ linear combination of coefficients must be chosen with d-wave symmetry. For case (2), i.e., d-wave-symmetric $\varphi^*_\alpha(k_x,k_y)\varphi_\beta(k_x,k_y)$, the correct linear combination has all positive expansion coefficients. Notably, for $\alpha = \beta$, the product of orbitals is invariant, so that any pair involving the same orbitals at neighboring sites must involve a linear combination of neighbors, which is odd in rotations by $\pi/2$. For example, in the anomalous matrix element F_{78} between the p_z orbitals of two Bi neighbors, the coefficient in the x direction has an opposite sign to that in the y direction.

V. DISCUSSION AND CONCLUSIONS

We emphasize that the logic of symmetry rules for the anomalous matrix elements is more complicated than that of the regular matrix elements. In particular, the nonvanishing tunneling channels can be determined through group theoretic considerations.[11,12] For example, because the rotational symmetry of the p_z orbitals of Bi and apical oxygen atoms differs from that of the $d_{x^2-y^2}$ orbital of the Cu *at the same horizontal position,* the corresponding off-diagonal term of the *regular* Green's function vanishes, inhibiting the corresponding tunneling channel. In contrast, coupling between electron and hole degrees of freedom via the gap matrix $\Delta_{\alpha\beta}$ leads to less obvious symmetry rules for the anomalous matrix elements: Now the quasiparticles are linear combinations of spin-up electrons and spin-down holes, and there is no simple rule for selecting the orbitals contributing to a chosen quasiparticle state. Hence, the p_z or d_{z^2} orbitals of Bi, O, or Cu atoms may couple to a $d_{x^2-y^2}$ orbital of a Cu atom at the same horizontal position, and the possibility of this coupling must be checked by considering the tensor form of Dyson's equation, as written out in Eq. (12), together with the transformation into the tight-binding basis of Eq. (14).

In summary, we have presented a comprehensive study of anomalous matrix elements of the Green's function derived from a realistic multiband model of Bi2212. The imaginary parts of these matrix elements describe the contributions of different orbitals to the coherence peaks involving the formation and breaking up of Cooper pairs. Although the pairing interaction is modeled by a local d-wave term in the Hamiltonian connecting only the $d_{x^2-y^2}$ orbitals of neighboring Cu atoms, the anomalous matrix elements display a longer range with induced superconductivity appearing at other sites and/or orbitals, including the second cuprate layer and the BiO/SrO overlayers. Our analysis delineates the precise routes through which the induced superconductivity in a complex cuprate system is transferred between various orbitals and sites.

ACKNOWLEDGMENTS

We acknowledge discussion with Matti Lindroos. This work is supported by the US Department of Energy under Contract No. DE-FG02-07ER46352, and benefited from the allocation of supercomputer time at NERSC and Northeastern University's Advanced Scientific Computation Center (ASCC). I.S. thanks Vilho, Yrjöja Kalle Väisälä Foundation for financial support. This work benefited from resources of the Institute of Advanced Computing, Tampere.

APPENDIX: SYMMETRY PROPERTIES OF REGULAR MATRIX ELEMENTS OF THE GREEN'S FUNCTION

This Appendix delineates the symmetry properties of the regular matrix elements of the normal and superconducting (SC) state Green's functions $G^0(\epsilon)$ and $G(\epsilon)$, respectively, which were seen in connection with Eq. (14) above to be important for understanding the nature of anomalous matrix elements. Taking the origin at the position of the zeroth atom, $G^0_{0\alpha j\beta}(\varepsilon)$ can be written as

$$\begin{aligned} G^0_{0\alpha j\beta}(\varepsilon) &= \sum_{\mathbf{k}} \langle 0\alpha|\mathbf{k}\rangle G^0(\mathbf{k},\varepsilon)\langle \mathbf{k}|j\beta\rangle \\ &= \sum_{k} e^{i\mathbf{k}\cdot\mathbf{R_j}} \varphi^*_\alpha(\mathbf{k})\varphi_\beta(\mathbf{k}) G^0(\mathbf{k},\varepsilon), \end{aligned} \quad (A1)$$

where

$$G^0(\mathbf{k},\varepsilon) = \frac{1}{\varepsilon - \varepsilon_k - \Sigma(\varepsilon)}. \quad (A2)$$

Because the Hamiltonian is invariant under rotations of $\pi/2$, the dispersion ε_k and $G^0(\mathbf{k},\varepsilon)$ are also invariant. This is true as well for the SC state regular Green's function because the self-energy in Eq. (A2) is augmented by an additional term $\Sigma^{\mathrm{BCS}} = \Delta_k G^0_h(\mathbf{k},\varepsilon)\Delta^\dagger_k$, which is rotationally invariant.[12] Because G^0 and G possess the same symmetry properties, in the following we only consider the symmetry properties of $G^0(\mathbf{k},\varepsilon)$.

Consider first the case where $R_j = (0,0,c)$. Then, $G^0_{0\alpha j\beta} \neq 0$ only if $\varphi^*_\alpha(\mathbf{k})\varphi_\beta(\mathbf{k})$ in Eq. (A1) is invariant under the in-plane operations of the symmetry group of the Hamiltonian. For example, a p_z orbital can have nonzero matrix elements with s, p_z, or d_{z^2} of an atom at the same horizontal position. But the matrix element between p_z and $d_{x^2-y^2}$ of atoms at the same horizontal position is zero. For $c = 0$, the matrix element is nonzero only if the orbitals are similar.

We next consider the case where there are four atoms around a central atom at the distance of the horizontal lattice constant a: $R_1 = (a,0,c)$, $R_2 = (0,a,c)$, $R_3 = (-a,0,c)$, and $R_4 = (0,-a,c)$. Changing the indices according to $1 \to 2 \to 3 \to 4 \to 1$ corresponds to rotations by $\pi/2$ in real space. The transformation $k_y \to k_x$ and $k_x \to -k_y$ represents the same rotation in k space. Now the phase factor $e^{ik\cdot R_j}$ has a fundamental effect on the symmetry behavior. Let us compare

cases $R_1 = (a,0,c)$ and $R_2 = (0,a,c)$ and check whether the sign of the sum changes. In the first instance we get

$$G^0_{0\alpha 1\beta}(\varepsilon) = \sum_{\mathbf{k}} e^{i(k_x a + k_z c)} \varphi^*_\alpha(k_x,k_y)\varphi_\beta(k_x,k_y) G^0(\mathbf{k},\varepsilon), \quad \text{(A3)}$$

while the second case gives

$$G^0_{0\alpha 2\beta}(\varepsilon) = \sum_{\mathbf{k}} e^{i(k_y a + k_z c)} \varphi^*_\alpha(k_x,k_y)\varphi_\beta(k_x,k_y) G^0(\mathbf{k},\varepsilon). \quad \text{(A4)}$$

Applying the transformation $k_y \to k_x$ and $k_x \to -k_y$ to Eq. (A4) yields

$$G^0_{0\alpha 2\beta}(\varepsilon) = \sum_{\mathbf{k}} e^{i(k_x a + k_z c)} \varphi^*_\alpha(-k_y,k_x)\varphi_\beta(-k_y,k_x) G^0(\mathbf{k},\varepsilon). \quad \text{(A5)}$$

Thus, it is the product $\varphi^*_\alpha(-k_y,k_x)\varphi_\beta(-k_y,k_x)$ that determines what happens under rotations of $\pi/2$. If this is equal to $\varphi^*_\alpha(k_x,k_y)\varphi_\beta(k_x,k_y)$, the matrix element does not change sign under rotations, otherwise $G^0_{0\alpha j\beta}$ changes sign under in-plane rotation of $\pi/2$. In particular, for $\alpha = \beta$, this term is invariant, but for $\alpha = p_z$ or d_{z^2} and $\beta = d_{x^2-y^2}$, there is a change of sign under rotation.

An equivalent approach is to consider a linear combination of orbitals $j\beta$,

$$|\phi\rangle = \sum_{j=1}^{4} c_j |j\beta\rangle. \quad \text{(A6)}$$

There is a nonzero regular matrix element $G^0_{0\alpha,\phi}$ only if $|\phi\rangle$ belongs to the same representation of the symmetry group of the Hamiltonian as orbital $|0\alpha\rangle$. The transformation of the expansion coefficients c_j follows directly from the transformation of $G^0_{0\alpha j\beta}$. For example, it is obvious that

$$G^0_{0\alpha,\phi} = \sum_{j=1}^{4} c_j G^0_{0\alpha j\beta}. \quad \text{(A7)}$$

Hence, if $\alpha = \beta = d_{x^2-y^2}$ and $j = 1,\ldots,4$ are defined as above, c_j must be a constant in order to keep the full symmetry of the group of the Hamiltonian, leading to

$$G^0_{0\alpha,\phi} \propto c_1 e^{ik_z c}[\cos(k_x a) + \cos(k_y a)]\left(k_x^2 - k_y^2\right)^2.$$

If, however, $\alpha = d_{z^2}$ and $\beta = d_{x^2-y^2}$, one must have $c_2 = c_4 = -c_1 = -c_3$, and then

$$G^0_{0\alpha,\phi} \propto c_1 e^{ik_z c}[\cos(k_x a) - \cos(k_y a)]\left(k_x^2 - k_y^2\right)\left(3k_z^2 - k^2\right),$$

which requires a change of sign of c_j's under rotations of $\pi/2$ in order to obtain an invariant matrix element.

*jouko.nieminen@tut.fi

[1] Ø. Fischer, M. Kugler, I. Maggio-Aprile, Chr. Berthod, and Chr. Renner, Rev. Mod. Phys. **79**, 353 (2007).

[2] K. McElroy, J. Lee, J. A. Slezak, D.-H. Lee, H. Eisaki, S. Uchida, and J. C. Davis, Science **309**, 1048 (2005).

[3] E. W. Hudson, K. M. Lang, V. Madhavan, S. H. Pan, H. Eisaki, S. Uchida, and J. C. Davis, Nature (London) **411**, 920 (2001).

[4] S. H. Pan, E. W. Hudson, K. M. Lang, H. Eisaki, S. Uchida, and J. C. Davis, Nature (London) **403**, 746 (2000).

[5] A. N. Pasupathy, A. Pushp, K. K. Gomes, C. V. Parker, J. Wen, Z. Xu, G. Gu, S. Ono, Y. Ando, and A. Yazdani, Science **320**, 196 (2008).

[6] H. Meissner, Phys. Rev. **117**, 672 (1960).

[7] P. G. de Gennes, Rev. Mod. Phys. **36**, 225 (1964).

[8] W. L. McMillan, Phys. Rev. B **175**, 537 (1968).

[9] C. V. Parker, A. Pushp, A. N. Pasupathy, K. K. Gomes, J. Wen, Z. Xu, S. Ono, G. Gu, and A. Yazdani, Phys. Rev. Lett. **104**, 117001 (2010).

[10] J. E. Hoffman, Physics **3**, 23 (2010).

[11] J. A. Nieminen, H. Lin, R. S. Markiewicz, and A. Bansil, Phys. Rev. Lett. **102**, 037001 (2009).

[12] J. Nieminen, I. Suominen, R. S. Markiewicz, H. Lin, and A. Bansil, Phys. Rev. B **80**, 134509 (2009).

[13] S. Sahrakorpi, M. Lindroos, R. S. Markiewicz, and A. Bansil, Phys. Rev. Lett. **95**, 157601 (2005); A. Bansil, M. Lindroos, S. Sahrakorpi, and R. S. Markiewicz, Phys. Rev. B **71**, 012503 (2005).

[14] R. S. Markiewicz and A. Bansil, Phys. Rev. Lett. **96**, 107005 (2006); Y. W. Li *et al.*, Phys. Rev. B **78**, 073104 (2008).

[15] Y. Tanaka, Y. Sakurai, A. T. Stewart, N. Shiotani, P. E. Mijnarends, S. Kaprzyk, and A. Bansil, Phys. Rev. B **63**, 045120 (2001); S. Huotari, K. Hamalainen, S. Manninen, S. Kaprzyk, A. Bansil, W. Caliebe, T. Buslaps, V. Honkimaki, and P. Suortti, *ibid.* **62**, 7956 (2000).

[16] B. Barbiellini, A. Koizumi, P. E. Mijnarends, W. Al Sawai, Hsin Lin, T. Nagao, K. Hirota, M. Itou, Y. Sakurai, and A. Bansil, Phys. Rev. Lett. **102**, 206402 (2009); Y. Li, P. A. Montano, B. Barbiellini, P. E. Mijnarends, S. Kaprzyk, and A. Bansil, J. Phys. Chem. Solids **68**, 1556 (2007).

[17] J. C. Campuzano, L. C. Smedskjaer, R. Benedek, G. Jennings, and A. Bansil, Phys. Rev. B **43**, 2788 (1991); P. E. Mijnarends, A. C. Kruseman, A. van Veen, H. Schut, and A. Bansil, J. Phys. Condens. Matter **10**, 10383 (1998).

[18] Our use of a relatively thin slab of seven layers is adequate for our purpose of exploring tunneling to the tip from the cuprate bilayer in the presence of BiO and SrO overlayers. Thicker slabs containing multiple unit cells will be needed for delineating c-axis coherence effects involving coupling between different cuprate bilayers (Ref. 19). Also, because our modeling involves BiO and SrO layers with the perfect bulk structure, it is not sensitive to effects of impurities in the surface layers. O, Ni, and Zn impurities have been shown to produce a variety of interesting features in the STS spectrum (Refs. 3, 4, and 20).

[19] E. J. Singley *et al.*, Phys. Rev. B **69**, 092512 (2004); T. Shibauchi and S. Horiuchi, Physica C **460–462**, 174 (2007); P. Spathis, S. Colson, F. Yang, C. J. van der Beek, P. Gierłowski, T. Shibauchi, Y. Matsuda, M. Gaifullin, M. Li, and P. H. Kes, Phys. Rev. B **77**, 104503 (2008).

[20] Y. He, T. S. Nunner, P. J. Hirschfeld, and H.-P. Cheng, Phys. Rev. Lett. **96**, 197002 (2006).

[21] V. Bellini, F. Manghi, T. Thonhauser, and C. Ambrosch-Draxl, Phys. Rev. B **69**, 184508 (2004).

[22] The Hamiltonian of Eq. (1) is appropriate for the overdoped regime considered here. In the underdoped system, effects of the pseudogap must of course also be included as, for example, in Refs. 23 and 24.

[23] T. Das, R. S. Markiewicz, and A. Bansil, Phys. Rev. B **81**, 174504 (2010); **77**, 134516 (2008).

[24] R. S. Markiewicz, S. Sahrakorpi, and A. Bansil, Phys. Rev. B **76**, 174514 (2007); S. Basak, Tanmoy Das, Hsin Lin, J. Nieminen, M. Lindroos, R. S. Markiewicz, and A. Bansil, *ibid.* **80**, 214520 (2009).

[25] Within the LDA, there is a weak hybridization between the Cu d and Bi p_z orbitals, which plays a significant role in producing the observed tunnel current.

[26] Doping-independent tight-binding parameters in the spirit of a rigid-band picture are implicit in the form of our Hamiltonian in Eq. (1). A more realistic treatment of doping effects on electronic states could be undertaken by using various approaches (see, e.g., Refs. 27–29). However, we expect the rigid-band model to be a good approximation for doping away from the Cu-O planes.

[27] A. Bansil, S. Kaprzyk, P. E. Mijnarends, and J. Tobola, Phys. Rev. B **60**, 13396 (1999); A. Bansil, Z. Naturforsch., A: Phys. Sci. **48**, 165 (1993); R. Prasad and A. Bansil, Phys. Rev. B **21**, 496 (1980); L. Schwartz and A. Bansil, *ibid.* **10**, 3261 (1974).

[28] S. N. Khanna, A. K. Ibrahim, S. W. McKnight, and A. Bansil, Solid State Commun. **55**, 223 (1985); L. Huisman, D. Nicholson, L. Schwartz, and A. Bansil, Phys. Rev. B **24**, 1824 (1981).

[29] H. Lin, S. Sahrakorpi, R. S. Markiewicz, and A. Bansil, Phys. Rev. Lett. **96**, 097001 (2006).

[30] J.-M. Tang and M. E. Flatté, Phys. Rev. B **66**, 060504(R) (2002); **70**, 140510(R) (2004).

[31] We have used a sparse Δ matrix limited to coupling between $d_{x^2-y^2}$ orbitals of neighboring Cu atoms only in order to make the relation between Δ and $\langle c_{\alpha\downarrow} c_{\beta\uparrow} \rangle$ tractable. A more general Δ matrix could be obtained via a self-consistent application of Eq. (2).

[32] Note that in order to properly describe the shape of the coherence peaks (Ref. 33) we would need to include explicit coupling to bosonic modes.

[33] See also, A. Fang, C. Howald, N. Kaneko, M. Greven, and A. Kapitulnik, Phys. Rev. B **70**, 214514 (2004).

[34] A. L. Fetter and J. D. Walecka, *Quantum Theory of Many-Particle Systems* (Dover, New York, 2003).

[35] T. N. Todorov, G. A. D. Briggs, and A. P. Sutton, J. Phys. Condens. Matter **5**, 2389 (1993).

[36] J. B. Pendry, A. B. Prêtre, and B. C. H. Krutzen, J. Phys. Condens. Matter **3**, 4313 (1991).

[37] For our illustrative purposes, we have taken the imaginary part of the self-energy in the overdoped regime to be of Fermi-liquid form (Ref. 12). A more realistic description would consider self-energy corrections to account for electron-electron (Ref. 23) and electron-phonon (Ref. 38) interaction effects.

[38] M. Hengsberger, D. Purdie, P. Segovia, M. Garnier, and Y. Baer, Phys. Rev. Lett. **83**, 592 (1999); S. LaShell, E. Jensen, and T. Balasubramanian, Phys. Rev. B **61**, 2371 (2000).

[39] J. Tersoff and D. R. Hamann, Phys. Rev. B **31**, 805 (1985).

[40] P. Sautet, Surf. Sci. **374**, 406 (1997).

[41] M. Magoga and C. Joachim, Phys. Rev. B **59**, 16011 (1999).

[42] By "rotationally invariant" we mean invariance to in-plane rotation only, e.g., d_{z^2} and p_z orbitals are rotationally invariant. Also, by d-wave symmetry we mean an odd parity with respect to rotations of $\pi/2$ around the z axis.